Meriolins, a New Class of Cell Death–Inducing Kinase Inhibitors with Enhanced Selectivity for Cyclin-Dependent Kinases

Karima Bettayeb,[1] Oscar M. Tirado,[2] Séverine Marionneau-Lambot,[3] Yoan Ferandin,[1] Olivier Lozach,[1] Jonathan C. Morris,[4] Silvia Mateo-Lozano,[2] Peter Drueckes,[5,6] Christoph Schächtele,[5] Michael H.G. Kubbutat,[5] François Liger,[7] Bernard Marquet,[7] Benoît Joseph,[7] Aude Echalier,[8] Jane A. Endicott,[8] Vicente Notario,[2] and Laurent Meijer[1]

[1]Centre National de la Recherche Scientifique, Cell Cycle Group & UPS2682, Station Biologique, Roscoff, Bretagne, France; [2]Laboratory of Experimental Carcinogenesis, Lombardi Comprehensive Cancer Center, Georgetown University Medical Center, Washington, District of Columbia; [3]Cancéropôle Grand Ouest, Nantes, France; [4]Department of Chemistry, School of Chemistry and Physics, University of Adelaide, Adelaide, Australia; [5]ProQinase GmbH, Freiburg, Germany; [6]Novartis Institutes for BioMedical Research, Expertise Platform Kinases, Basel, Switzerland; [7]ICBMS, UMR 5246, Université Lyon 1, Laboratoire de Chimie Organique 1, Villeurbanne, France; and [8]University of Oxford, Laboratory of Molecular Biophysics, Department of Biochemistry, Oxford, United Kingdom

Abstract

Protein kinases represent promising anticancer drug targets. We describe here the meriolins, a new family of inhibitors of cyclin-dependent kinases (CDK). Meriolins represent a chemical structural hybrid between meridianins and variolins, two families of kinase inhibitors extracted from various marine invertebrates. Variolin B is currently in preclinical evaluation as an antitumor agent. A selectivity study done on 32 kinases showed that, compared with variolin B, meriolins display enhanced specificity toward CDKs, with marked potency on CDK2 and CDK9. The structures of pCDK2/cyclin A/variolin B and pCDK2/cyclin A/meriolin 3 complexes reveal that the two inhibitors bind within the ATP binding site of the kinase, but in different orientations. Meriolins display better antiproliferative and proapoptotic properties in human tumor cell cultures than their parent molecules, meridianins and variolins. Phosphorylation at CDK1, CDK4, and CDK9 sites on, respectively, protein phosphatase 1α, retinoblastoma protein, and RNA polymerase II is inhibited in neuroblastoma SH-SY5Y cells exposed to meriolins. Apoptosis triggered by meriolins is accompanied by rapid Mcl-1 down-regulation, cytochrome *c* release, and activation of caspases. Meriolin 3 potently inhibits tumor growth in two mouse xenograft cancer models, namely, Ewing's sarcoma and LS174T colorectal carcinoma. Meriolins thus constitute a new CDK inhibitory scaffold, with promising antitumor activity, derived from molecules initially isolated from marine organisms. [Cancer Res 2007;67(17):8325–34]

Introduction

Altered protein phosphorylation is a frequent feature in numerous human diseases. This last decade has therefore witnessed considerable efforts to identify, optimize, and evaluate pharmacologic inhibitors of protein kinases (reviews in refs. 1, 2). Currently, ~60 kinase inhibitors are undergoing clinical evaluation against cancers, inflammation, diabetes, and neurodegenerative diseases.

Among the 518 human kinases, cyclin-dependent kinases (CDK) have attracted considerable interest given their involvement in many essential physiologic pathways and aberrant activities in multiple human diseases, especially in cancer and neurodegenerative diseases (review in ref. 3). Consequently, many pharmacologic inhibitors of CDKs have been found to display promising antitumor and/or neuroprotective activities (reviews in refs. 4–8). To our knowledge, eight CDK inhibitors are currently undergoing clinical evaluation as anticancer drugs [flavopiridol (Alvocidib), *R*-roscovitine (CYC202, Seliciclib), R547, SNS-032, PD-0332991, AZD5438, AG-024322 and AT7519]. All CDK inhibitors identified to date are ATP-competitive, and many have been co-crystallized with a CDK target (review in ref. 1). The selectivity of these pharmacologic inhibitors is a matter of extensive investigation using a wide variety of methods (review in ref. 9). Although a few kinase inhibitors are rather unselective (like staurosporine), many display a definite specificity profile, but all inhibit several kinases. For example, many CDK inhibitors also inhibit glycogen synthase kinase-3 (GSK-3; ref. 10) and sometimes casein kinase 1 (CK1). Multitarget inhibitors may find appropriate medicinal use because they are less likely to allow resistance to develop.

We recently identified meridianins, a family of 3-(2-aminopyrimidine)indoles, as a promising kinase-inhibitory scaffold (11). Meridianins are natural products initially extracted from *Aplidium meridianum*, an Ascidian from the South Atlantic (12). Meridianin derivatives have been synthesized by various groups (13–15). Although some meridianins inhibit various kinases such as CDKs, GSK-3, cyclic nucleotide-dependent kinases, and CK1, they displayed modest antiproliferative effects. Meridianins share some structural similarity with variolins, another family of marine natural compounds containing a central pyrido[3′,2′:4,5]pyrrolo[1,2-*c*]pyrimidine core substituted with a 2-aminopyrimidine ring. Variolins were initially extracted from *Kirkpatrickia variolosa*, a rare Antarctic sponge (16, 17). Total synthesis by Morris (18, 19) and others (20, 21) allowed easy access to the variolins. Variolin B and deoxyvariolin B (PM01218) display potent cytotoxicity against several human cancer cell lines (17, 22, 23); as a result, PM01218 is being investigated by PharmaMar as a potential antitumor drug. Recently, as this work was in progress, variolin B and deoxyvariolin B were reported to inhibit CDKs (23).

In this article, we have exploited the chemical similarity between meridianins and variolins to synthesize a hybrid structure, the meriolins. Surprisingly, meriolins display potent inhibitory activity and relative selectivity toward CDKs and also exhibit better

Note: Supplementary data for this article are available at Cancer Research Online (http://cancerres.aacrjournals.org/).

Requests for reprints: L. Meijer, Centre National de la Recherche Scientifique, Cell Cycle Group & UPS2682, Station Biologique, B.P. 74, 29682 Roscoff Cedex, Bretagne, France. Phone: 330-298-29-23-39; Fax: 330-298-29-23-42; E-mail: meijer@sb-roscoff.fr.

doi:10.1158/0008-5472.CAN-07-1826

antiproliferative and proapoptotic properties in cell cultures than their "inspirational parent" molecules. Meriolins are particularly potent inhibitors of CDK2 and CDK9. The crystal structures of meriolin 3 and variolin B in complex with CDK2/cyclin A revealed that the two molecules bind in very different orientations in the ATP-binding pocket of the kinase. Meriolins prevent phosphorylation at CDK1-, CDK4-, and CDK9-specific sites in neuroblastoma SH-SY5Y cells and induce the rapid degradation of the survival factor Mcl-1. Meriolin 3 potently inhibits tumor growth in two mouse xenograft models: Ewing's sarcoma and LS174T colorectal carcinoma. Meriolins thus constitute a new kinase-inhibitory scaffold with promising antitumor activity.

Materials and Methods

Chemistry

Synthesis of meridianins, variolins, and meriolins. Meridianins A and G were synthesized as described previously (15). Variolin B and deoxyvariolin B were synthesized in eight and six steps, respectively, as described previously (18, 19). The synthesis of meriolins will be described in detail in a separate article.[9] Briefly, meriolins were prepared as follows. Acylation of 7-azaindole derivatives (7-azaindole, 4-methoxy-7-azaindole, and 4-ethoxy-7-azaindole) in the presence of acetic anhydride and trifluoroacetic acid afforded the 3-acetyl-7-azaindole derivatives in 55% to 84% yield. N-benzenesulfonylation of the latter compounds was carried out in the presence of benzenesulfonyl chloride and sodium hydride in tetrahydrofuran to give 3-acetyl-1-benzenesulfonyl-7-azaindole derivatives in 68% to 90% yield. Treatment of the protected 7-azaindoles with *N,N*-dimethylformamide dimethyl acetal in *N,N*-dimethylformamide afforded the corresponding enaminones in 68% to 78% yield. Final formation of the pyrimidic nucleus occurred by heating of enaminones in the presence of guanidine HCl and anhydrous potassium carbonate in 2-methoxyethanol to afford meriolins 1, 3, and 4 in 63% to 75% yield. O-demethylation of meriolin 3 was done in 48% hydrobromic acid/acetic acid to afford meriolin 2 in 90% yield.

Crystallography

Expression, purification, and co-crystallization of human CDK2/cyclin A with meriolin 3 and variolin B. Thr^{160}-phosphorylated CDK2/cyclin A (pCDK2/cyclin A) was purified as described previously (24) and concentrated to 13 mg/mL in 40 mmol/L HEPES (pH, 7.0), 200 mmol/L NaCl, 0.01% monothioglycerol. The protein solution was incubated for 20 min on ice with meriolin 3 (1.8 mmol/L) or variolin B (2.0 mmol/L) before setting up hanging-drop crystallization trials. The reservoir solution contained 0.6 to 0.8 mol/L KCl, 0.9 to 1.2 mol/L $(NH_4)_2SO_4$, and 100 mmol/L HEPES (pH, 7.0). Orthorhombic crystals grew within 3 weeks at 4°C. Crystals were briefly soaked in 8 mol/L sodium formate before being cryo-cooled in liquid nitrogen.

X-ray crystallography data collection and processing, structure solution, and refinement. Data were collected from a single crystal on ESRF ID14-EH-2 beamline at 100K. Data processing and integration were carried out using MOSFLM and SCALA (25). The structures were solved by molecular replacement with MOLREP using a well-refined structure of pCDK2/cyclin A[10] as the search model. Two pCDK2/cyclin A heterodimers were found in the asymmetrical unit. Strong electron density corresponding to the bound inhibitor was seen at the ATP site after rigid body refinement of the two structures. Inhibitor model building and library generation for the two inhibitors were done using the CCP4 software suite (25). Alternate cycles of rebuilding in Coot (26) and refinement in Refmac (27) were carried out to obtain the final models.

[9] A. Echalier et al., submitted.
[10] Unpublished results.

Protein Kinase Assays

Buffers. Buffer A: 10 mmol/L $MgCl_2$, 1 mmol/L EGTA, 1 mmol/L DTT, 25 mmol/L Tris-HCl (pH, 7.5), 50 μg heparin/mL. Buffer C: 60 mmol/L β-glycerophosphate, 15 mmol/L *p*-nitrophenylphosphate, 25 mmol/L MOPS (pH, 7.2), 5 mmol/L EGTA, 15 mmol/L $MgCl_2$, 1 mmol/L DTT, 1 mmol/L sodium vanadate, 1 mmol/L phenylphosphate.

Kinase preparations and assays. Kinase activities were assayed in buffer A or C at 30°C at a final ATP concentration of 15 μmol/L. Blank values were subtracted, and activities were expressed in percent of the maximal activity, i.e., in the absence of inhibitors. Controls were done with appropriate dilutions of DMSO.

CDK1/cyclin B (M phase starfish oocytes, native) and *CDK5/p25* (human, recombinant) were prepared as previously described (10). Kinase activity was assayed in buffer C, with 1 mg histone H1/mL, in the presence of 15 μmol/L [γ-^{33}P] ATP (3,000 Ci/mmol; 10 mCi/mL) in a final volume of 30 μL. After 30 min incubation at 30°C, 25-μL aliquots of supernatant were spotted onto 2.5 × 3-cm pieces of Whatman P81 phosphocellulose paper, and 20 s later, the filters were washed five times (for at least 5 min each time) in a solution of 10 mL phosphoric acid/L of water. The wet filters were counted in the presence of 1 mL ACS (Amersham) scintillation fluid.

CDK2/cyclin A (human, recombinant, expressed in insect cells) was assayed as described for CDK1/cyclin B.

CDK9/cyclin T (human, recombinant, expressed in insect cells) was assayed as for CDK1/cyclin B using a pRB fragment (amino acids 773–928; 3.5 μg/assay) as substrate.

GSK-3α/β (porcine brain, native, affinity purified) was assayed as described for CDK1, but in buffer A and using a GSK-3–specific substrate (GS-1: YRRAAVPPSPSLSRHSSPHQSpEDEEE; Sp stands for phosphorylated serine; ref. 28).

CK1δ/ε (porcine brain, native, affinity purified) was assayed as described for CDK1, but using the CK1-specific peptide substrate RRKHAAIGSpAY-SITA (29).

ProQinase protein kinase assays. All protein kinases were expressed in Sf9 insect cells as human recombinant glutathione *S*-transferase-fusion proteins or His-tagged proteins by means of the baculovirus expression system. Kinases were purified and assayed as described (28; Supplementary Materials).

Cell Biology

Antibodies and chemicals. AcDEVDafc and Q-VD-OPh were purchased from MPbiomedicals. Cell Titer 96 containing the MTS reagent and CytoTox 96 kits were purchased from Promega. The protease inhibitor cocktail was from Roche. Unless otherwise stated, the nonlisted reagents were from Sigma.

Monoclonal antibody against actin was obtained from Calbiochem. Monoclonal antibodies against cytochrome *c* and retinoblastoma protein (Rb) were purchased from BD Biosciences. Polyclonal antibody against phospho-Ser^{249}/Thr^{252}-Rb was provided by Biosource. Polyclonal antibody against phospho-Thr^{320}-protein phosphatase 1α (PP1α) and monoclonal antibody against caspase-9 were from Cell Signaling. Polyclonal antibodies against RNA polymerase II and phospho-Ser^2-RNA polymerase II were supplied by Covance Research Products. Polyclonal antibody against Mcl-1 was obtained from Santa Cruz Biotechnology.

Cell lines and culture conditions. SH-SY5Y human neuroblastoma, Huh7 human hepatocarcinoma and LS 174T human colorectal adenocarcinoma cell lines were grown in DMEM (Invitrogen). The HCT116 human colorectal carcinoma cell line was grown in McCoy's 5a medium from the American Type Culture Collection. The F1 rat biliary epithelial cell line was grown on Williams' Medium E from Invitrogen supplemented with 2 mmol/L L-glutamine from Lonza. The HEK 293 human embryonic kidney cell line was grown in MEM from Invitrogen. Human foreskin primary fibroblasts (kindly provided by Dr. Gilles Ponzio, Faculté de Médecine, INSERM U634, Nice, France) were grown in DMEM supplemented with 2 mmol/L L-glutamine and 20 mmol/L HEPES. All the media were supplemented with antibiotics (penicillin-streptomycin) from Lonza and 10% volume of FCS from Invitrogen. Cells were cultured at 37°C with 5%

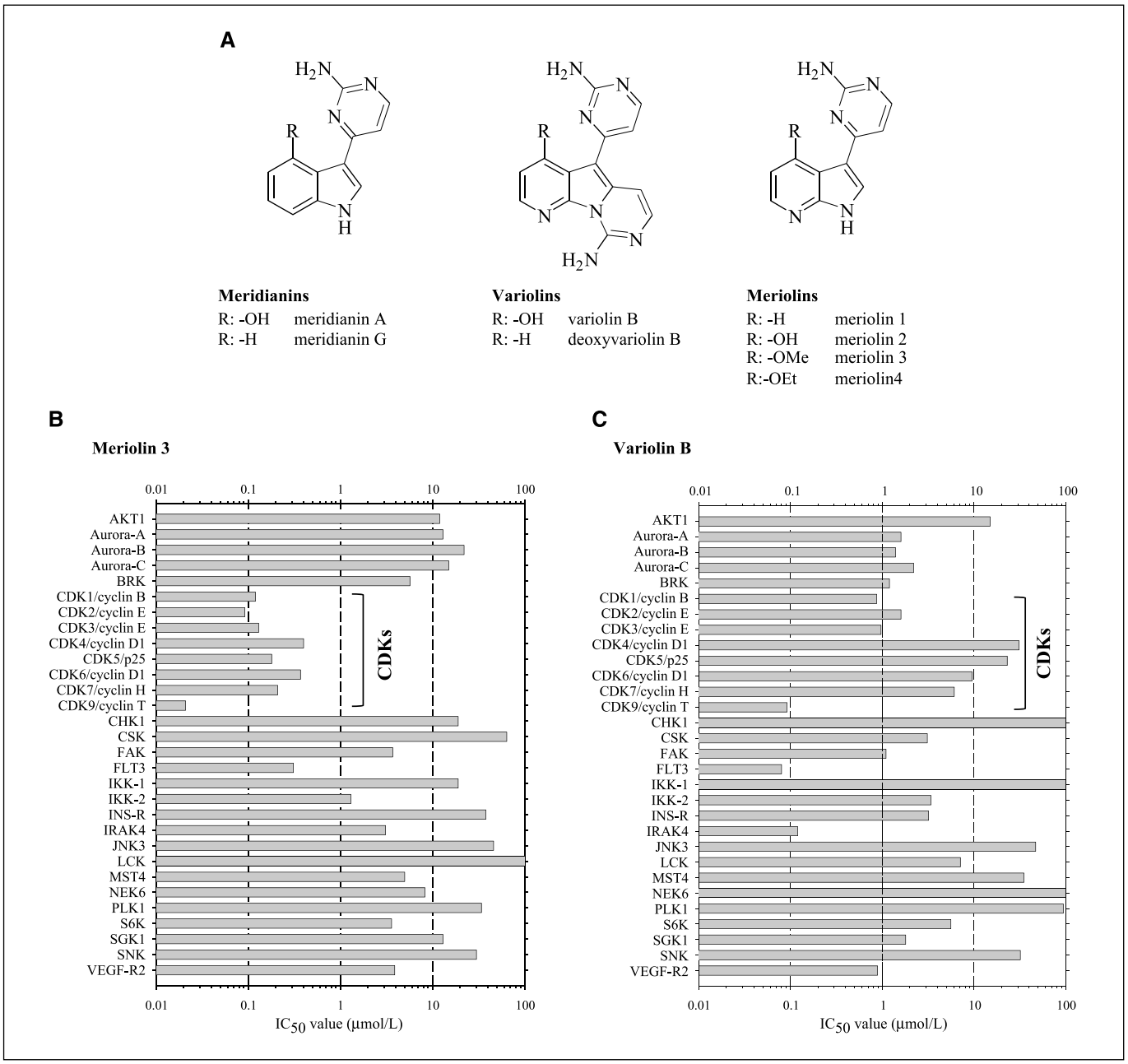

Figure 1. *A,* structures of meridianins, variolins, and meriolins. Selectivity of meriolin 3 (*B*) and variolin B (*C*). The two latter compounds were run at increasing concentrations on a ProQinase selectivity panel of 30 kinases. IC_{50} values are presented in micromoles per liter. ATP concentration used in the kinase assays was 1 μmol/L.

CO_2. Drug treatments were done on exponentially growing cultures at the indicated time and concentrations. Control experiments were carried out using appropriate dilutions of DMSO. KMS-11, multiple myeloma adherent cell line, and GBM, a multiform glioblastoma primary culture cells were cultured in RPMI 1640 supplemented, respectively, with 5% or 10% fetal calf serum, 2 mmol/L glutamine, antibiotics (100 IU/mL penicillin and 100 μg/mL streptomycin), and 10 μmol/L 2-β-mercaptoethanol (Life Technologies). Cells were subcultured at confluency after dispersal with 0.025% trypsin in 0.02% EDTA. Their survival was estimated by the neutral red uptake assay.[9]

Cell death and cell viability assessments. Cell viability was determined by measuring the reduction of 3-(4,5-dimethylthiazol-2-yl)-5-(3-carboxymethoxyphenyl)-2-(4-sulfophenyl)-2*H*-tetrazolium (MTS). Cell death was determined by measuring the level of lactate dehydrogenase (LDH) activity released upon cell lysis. Both procedures have been previously described in detail (30).

Caspase assay. Caspase activity was measured by determining the fluorescence released from the AcDEVDafc synthetic substrate after its direct addition to the culture medium, detergent lysis, and incubation at 37°. This method is devised for a 96-multiwell plate format. It allows kinetic determinations of caspase activation and the characterization of multiple drugs simultaneously (30).

Electrophoresis and Western blotting. Cells were resuspended and lysed in homogenization buffer [60 mmol/L β-glycerophosphate, 15 mmol/L *p*-nitrophenyl phosphate, 25 mmol/L MOPS (pH, 7.2), 15 mmol/L EGTA, 15 mmol/L $MgCl_2$, 1 mmol/L DTT, 1 mmol/L sodium vanadate, 1 mmol/L NaF, 1 mmol/L phenylphosphate, 0.1% Nonidet P-40, and protease inhibitor cocktail] and sonicated. After centrifugation (14,000 rpm for 15 min at 4°C),

Table 1. Effects of meridianins, variolins, and meriolins on six protein kinases and on the survival of neuroblastoma SH-SY5Y cells (*A*) and effects of meriolin 3 on the survival of various cell lines (*B*)

A

Compound	CDK1	CDK2	CDK5	CDK9	GSK3	CK1	SH-SY5Y
Meridianin A	2.50	3.10	3.00	2.40	1.30	1.10	> 30.00
Meridianin G	150.00	>10	140.00	>10	350.00	9.00	>30.00
Variolin B	0.06	0.08	0.09	0.026	0.07	0.005	0.24
Deoxyvariolin B	0.34	0.21	0.43	0.041	0.71	0.022	0.22
Meriolin 1	0.78	0.09	0.51	0.026	0.63	0.20	0.67
Meriolin 2	0.057	0.018	0.050	0.018	0.40	0.05	0.41
Meriolin 3	0.17	0.011	0.17	0.006	0.23	0.20	0.073
Meriolin 4	0.01	0.007	0.005	0.007	0.03	0.10	0.081

B

Cell line	Cell survival (IC_{50}, μmol/L; MTS reduction)
LS 174T (colorectal adenocarcinoma)	0.13
HCT116 (colon)	0.94
KMS-11 (myeloma)	0.12
GBM (glioma)	0.14
Huh7 (hepatoma)	0.12
F1 (hepatoma)	0.26
SH-SY5Y (neuroblastoma)	0.072
HEK293 (embryon kidney)	0.38
Human foreskin fibroblasts	8.00

NOTE: (A) Compounds were tested at various concentrations on CDK1/cyclin B, CDK2/cyclin A, CDK5/p25, CDK7/cyclin H, CDK9/cyclin T, GSK-3α/β, and CK1δ/ε as described in Materials and Methods. IC_{50} values, calculated from the dose-response curves (average of triplicate values), are reported in micromoles per liter (data for meridianins from ref. 19). The compounds were tested at various concentrations for their effects on SH-SY5Y cells survival after 48 h incubation as estimated using the MTS reduction assay. IC_{50} values, calculated from the dose-response curves, are reported in μmol/L. (B) Meriolin 3 was tested at various concentrations for its effects on nine different cell lines. Cell survival was estimated 48 h after the addition of meriolin 3 using the MTS reduction assay. IC_{50} values (average of triplicate values) are reported in micromoles per liter.

the protein concentration was determined in the supernatants by the Bradford protein assay (Bio-Rad). To study cytochrome *c* release from the mitochondria, a 0.05% digitonin cytosolic extraction was done (30).

Whole cell extracts were prepared in buffer containing 100 mmol/L Tris-HCl (pH, 6.8), 1 mmol/L EDTA, 2% SDS, and protease inhibitor cocktail. Following heat denaturation for 5 min, proteins were separated on 10% or 7% NuPAGE pre-cast Bis-Tris or Tris-acetate polyacrylamide mini gels (Invitrogen) with MOPS SDS (all but cytochrome *c*, RNA polymerase II, and phospho-Ser^2-RNA polymerase II Western blots), MES SDS (cytochrome *c*), or Tris-acetate SDS (RNA polymerase II and phospho-Ser^2-RNA polymerase II) running buffer depending on protein size. Proteins were transferred to 0.45-μm nitrocellulose filters (Schleicher and Schuell). These were blocked with 5% low-fat milk in TBS–Tween 20, incubated for 1 h with antibodies (anti-actin: 1:2,000) or overnight at 4°C (cytochrome *c*: 1:500), Rb (1:500), phospho-Rb (1:500), phospho-Thr^{320}-PP1α (1:1,000), RNA polymerase II (1:500), phospho-Ser^2-RNA polymerase II (1:500), Mcl-1 (1:500), and caspase-9 (1:1,000) and analyzed by enhanced chemiluminescence (ECL, Amersham).

In vivo Antitumor Activity

Ewing's sarcoma. Experiments to evaluate the antitumor activity of meriolin 3 were carried out essentially as described (31) under protocols approved by the Georgetown University Animal Care and Use Committee, using immunodeficient male (5–6 weeks old) athymic nude (BALB/c *nu/nu*) mice purchased from the U.S. National Cancer Institute, which were housed in the animal facilities of the Georgetown University Division of Comparative Medicine. Mice were injected s.c. into the right posterior flank with 4×10^6 A4573 Ewing's sarcoma cells in 100 μL of Matrigel basement membrane matrix (BD Biosciences). Once tumors reached a mean volume of about 195 mm^3, mice were randomized into two groups (six animals per group), and treatment was initiated. One group was treated with meriolin 3, dissolved in DMSO, and given as a single daily i.p. injection, at a dose of 1 mg/kg, for either 5 days or two 5-day series with a 2-day break in between. The control group received i.p. injections of DMSO following an identical schedule. Tumor growth was followed for up to 4 weeks after the first injection. Tumor volumes were calculated by the formula $V = (1/2)a \times b^2$, where a is the longest tumor axis, and b is the shortest tumor axis. Whenever tumors reached the maximum volume allowed by institutional tumor burden guidelines, animals were sacrificed by asphyxiation with CO_2. Tumors were immediately excised from euthanized animals and measured. Data are given as mean ± SD. Statistical analysis of differences between groups was done by a one-way ANOVA, followed by an unpaired Student's t test.

LS174T colorectal carcinoma. The antitumor activity of meriolin 3 was investigated by protocols approved by the Cancéropole Grand-Ouest Animal Care and Use Committee using immunodeficient female (5 weeks old) athymic nude (NMRI) mice purchased from Janvier. Mice were injected s.c. into the right flank with 4×10^6 colorectal LS174T cells in 100 μL of RPMI (Invitrogen). After 8 days, mice were randomized into three groups (five animals per group), and treatment was initiated. Meriolin 3, dissolved

in 30% DMSO in 0.9% NaCl, was given as a single daily i.p. injection at a dose of 2 or 5 mg/kg for two 5-day series with a 2-day break in between. The control group received i.p. injections of DMSO/NaCl following an identical schedule. Tumor sizes were measured daily. Tumor volumes were calculated by the formula $V = (1/2)a \times b^2$, where a is the longest tumor axis, and b is the shortest tumor axis. Data are given as mean ± SD. Whenever tumors reached the maximum volume allowed by institutional tumor burden guidelines (3,000 mm^3), animals were sacrificed by cervical dislocation. Animals were autopsied, and organs were examined macroscopically.

Results

Meriolins inhibit protein kinases, with selectivity toward CDKs. Both meridianins (11) and variolins (17, 22, 23) show distinct antiproliferative and proapoptotic activities. These effects may be correlated with their inhibitory activities toward CDKs and other protein kinases (11, 23). The chemical similarity between meridianins and variolins prompted us to synthesize an aza-indole hybrid structure, which we designated as a meriolin (Fig. 1*A*). Representatives of the three chemical families were initially tested on six purified protein kinases (CDK1/cyclin B, CDK2/cyclin A, CDK5/p25, CDK9/cyclin T, GSK-3α/β and CK1δ/ε; Table 1*A*). The moderate activity of meridianins (11) was confirmed. Variolin B was identified as a potent inhibitor of all CDKs and GSK-3, whereas deoxyvariolin B was 5- to 10-fold less potent. Interestingly, variolin B and deoxyvariolin B were very potent inhibitors of CK1, in fact, more potent than all reported CK1 inhibitors (29). Meriolins were very potent inhibitors of CDKs, GSK-3, and CK1. CDK2 and CDK9 seemed to be particularly sensitive to meriolins.

To evaluate their selectivity, we tested meriolin 3 and variolin B on a selection of 30 kinases from the ProQinase selectivity panel (Fig. 1*B* and *C*). The highest inhibitory activity of meriolin 3 was mostly restricted to CDKs, CDK9 being particularly sensitive under these conditions. Inhibitory activity was observed at higher doses for other kinases (Fig. 1). In contrast, variolin B did not display such a striking selectivity for CDKs, although CDK9 was also a good target.

Meriolin 3–CDK2/cyclin A and variolin B–CDK2/cyclin A co-crystal structures. We next investigated the molecular mechanism of action of meriolin 3 and variolin B by co-crystallization with pCDK2/cyclin A (Fig. 2). A full description of the co-crystal structures and comparison with previously described CDK2/inhibitors structures will be presented elsewhere.[9] Meriolin and variolin B both occupy the kinase ATP binding site located between the smaller NH_2-terminal and large COOH-terminal lobes (Fig. 2*A*). Meriolin 3 makes two hydrogen bonds to the CDK2 backbone within the hinge sequence that links the two lobes of the kinase: it accepts a hydrogen bond from the backbone nitrogen of Leu^{83} and donates a hydrogen bond to the backbone oxygen of Glu^{81} (Fig. 2*B*). In addition, meriolin 3 makes two hydrogen bonds with the side chains of Lys^{33} and Glu^{51} (Fig. 2*B*).

Although variolin B and meriolin 3 share a substantial portion of their scaffold, the two molecules are oriented differently within the ATP binding cleft. Variolin B, like meriolin 3, makes two equivalent hydrogen bonds with the CDK2 hinge and also interacts with the side chain of Lys^{33} through its hydroxyl group. In addition, two ordered water molecules (Fig. 2*B, red stars*) are discernible in the variolin B–bound active site, and one interacts with Ile^{10} main chain amine. However, the presence of a third ring fused to the variolin B indole creates a planar structure that is too large to be accommodated at the back of the ATP binding site if variolin B were to adopt the meriolin 3 binding mode. As a result, the indole moiety common to both inhibitors is flipped 180° between the two bound structures.

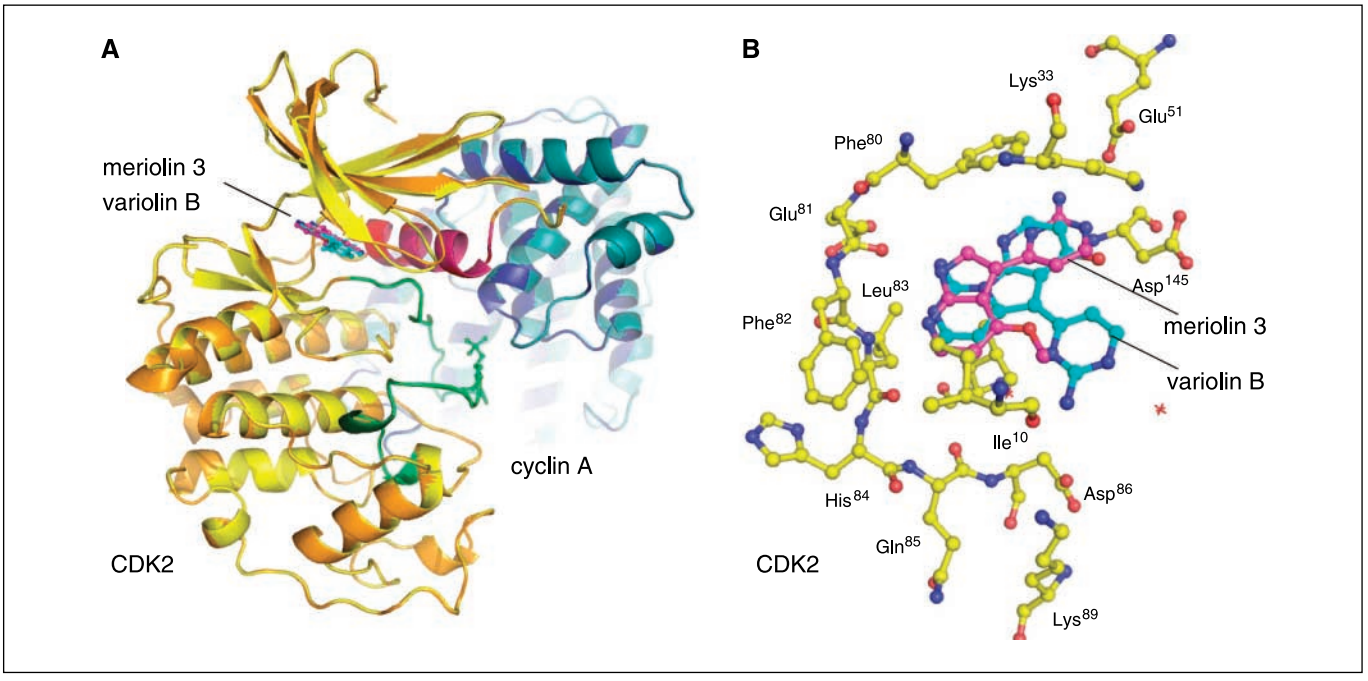

Figure 2. Co-crystal structure of meriolin 3 and variolin B with CDK2/cyclin A. *A,* structure of pCDK2/cyclin A in ribbon diagram representation. *Yellow,* CDK2 (with variolin *B*) and in orange (with meriolin 3). The PSTAIRE helix (residues 45–57) is shown in magenta and the activation segment (residues 145–172) is in green. Cyclin A is shown in blue for variolin B structure and in cyan for meriolin 3 structure. Meriolin 3 is shown in magenta at the ATP binding site and variolin B in cyan. Meriolin 3, variolin B, and phospho-Thr^{160} are shown in ball-and-stick representation. *B,* details of the interactions of meriolin 3 and variolin B with the ATP binding pocket of pCDK2/cyclin A. Meriolin 3, variolin B, and selected residues of CDK2 (from meriolin 3 structure) are shown in ball-and-stick representation in magenta, cyan, and yellow, respectively.

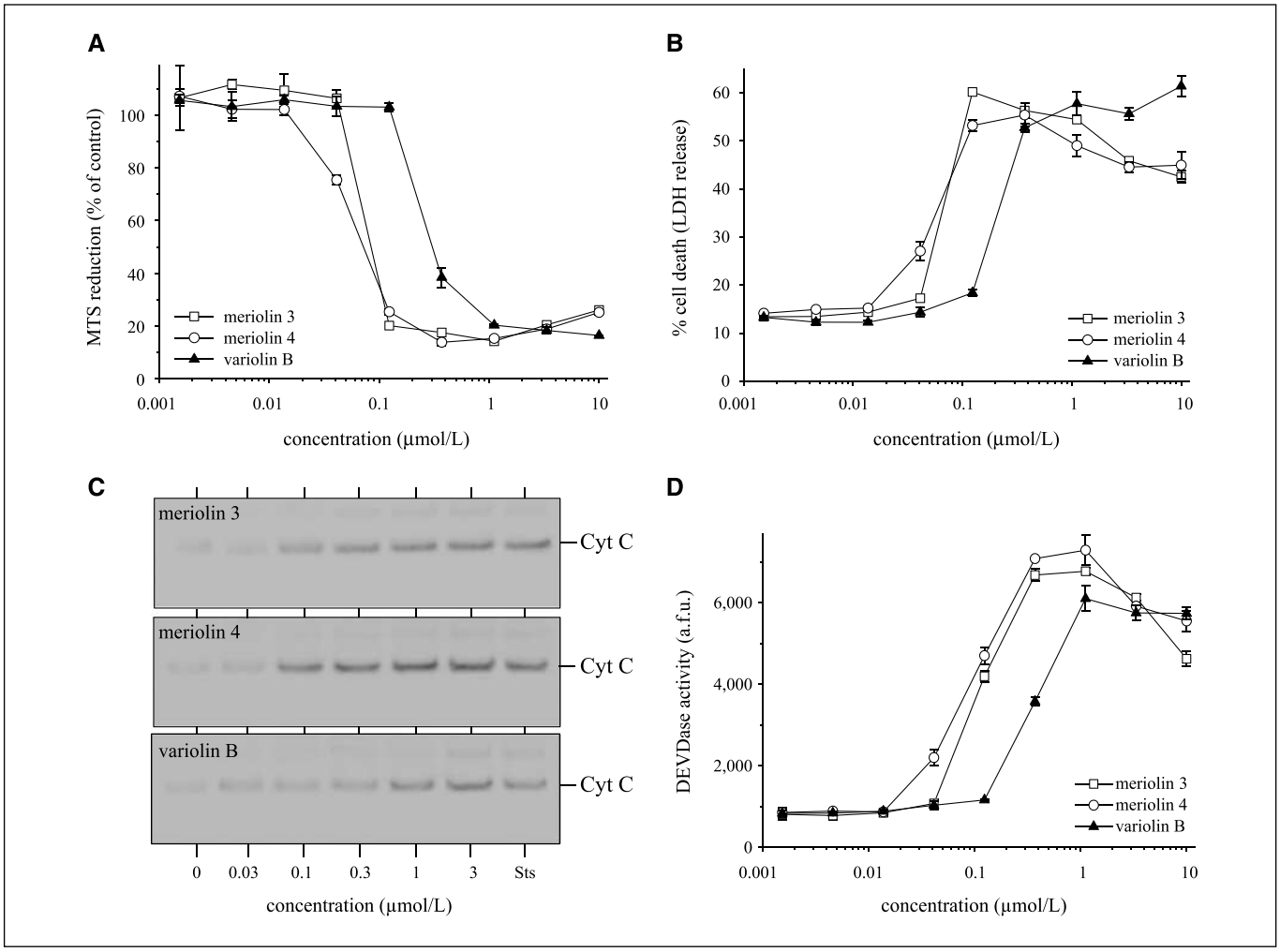

Figure 3. Induction of cell death in SH-SY5Y cells by meriolins 3 and 4 and variolin B. *A,* SH-SY5Y cells were exposed for 48 h to increasing concentrations of the three compounds. Cell survival was estimated by the MTS reduction assay and is expressed in % of survival in untreated cells. Average ± SE of one out of three independent experiments, done in triplicates. *B,* a similar experiment was done, but LDH release was assayed 24 h after the addition of the compounds. Average ± SE of three independent measurements per experiment. *C,* Induction of the apoptosis pathway: SH-SY5Y cells were exposed for 24 h to increasing concentrations of the three compounds. Cells were then harvested and fractionated into a nuclear pellet and a cytoplasmic supernatant. The latter was resolved by SDS-PAGE followed by Western blotting using an anti-cytochrome *c* antibody. *D,* induction of caspases activation. Cells were exposed for 24 h to increasing concentrations of the three compounds. DEVDase activity was measured as arbitrary fluorescence units. *Points,* mean of at least three independent determinations; *bars,* SE. *Sts,* staurosporine 0.25 μmol/L.

Meriolins induce apoptotic cell death. We next compared the three families of compounds for their ability to induce cell death in neuroblastoma SH-SY5Y cells as measured with an MTS reduction assay (Table 1*A*; Fig. 3*A*). Because MTS reduction is occasionally observed under conditions in which cell death does not occur, we also used an independent cell death assay, the lactate dehydrogenase (LDH) release assay (Fig. 3*B*). Dose-response curves showed that meriolins are more potent than variolin B in terms of the concentration required to reduce cell survival (MTS reduction; Table 1*A*; Fig. 3*A*) or in terms of cell death induction (LDH release; Fig. 3*B*).

To confirm that the induction of cell death by meriolins was not a specific property of SH-SY5Y cells, we tested meriolin 3 on different human cancer cell lines (Table 1*B*). A 48-h exposure induced a dose-dependent reduction of cell survival in all cell lines. However, normal human foreskin primary fibroblasts were much less sensitive.

Cell death induced by meriolins and variolin B was accompanied by a dose-dependent release of cytochrome *c* (Fig. 3*C*) and activation of effector caspases (Fig. 3*D*). Meriolins were more potent than variolin B at triggering both cytochrome *c* release and caspase activation.

We next analyzed the effects of meriolins 3 and 4 and variolin B on the phosphorylation of various proteins at CDK-specific sites. Although meriolins induced a modest reduction in Rb levels (Supplementary Figure), they strongly and dose-dependently reduced Rb phosphorylation at CDK4-specific sites (Ser^{249}/Thr^{252}; ref. 32; Fig. 4*A*). PP1α phosphorylation by CDK1 at Thr^{320} is a reported marker of CDK1 activity (33, 34). Meriolins were very potent at inhibiting CDK1-specific Thr^{320} phosphorylation of PP1α in a dose-dependent manner, whereas variolin B was only active at the highest (1 μmol/L) concentration tested (Fig. 4*B*). RNA polymerase II is phosphorylated by CDK9 on Ser^{2}. Although only meriolin 4 induced a modest reduction in RNA polymerase II level (Supplementary Figure), all three compounds inhibited CDK9-specific Ser^{2} phosphorylation of RNA polymerase II in a dose-dependent manner (Fig. 4*C*). Meriolins were more active than

variolin B. We next tested the effects of the three compounds on the level of the short-lived survival factor Mcl-1 (Fig. 4*D*). Western blot analysis showed that meriolins induced an almost complete disappearance of Mcl-1, whereas variolin B was essentially inactive.

***In vivo* antitumor activity of meriolin 3.** A nude mouse tumor xenograft model system (31) was used to evaluate the antitumor effect of meriolin 3 *in vivo*. Results showed that as early as 3 days after treatment initiation, meriolin 3 had slowed tumor growth by about 54% (Fig. 5*A*). Five days later (day 14), when tumors in control animals reached an average volume about 2,000 mm^3, and animals had to be sacrificed, tumors in meriolin 3–treated animals had reached an average volume of only $\sim$700 mm^3 ($\sim$65% tumor growth inhibition). The inhibitory effect of meriolin 3 on tumor growth was also manifested by the fact that tumors in meriolin 3–treated animals took an additional period of about 20 days to reach the maximum volume allowed by institutional tumor burden standards (Fig. 5*A*). We used a second nude mouse tumor xenograft model to confirm these *in vivo* antitumor effects (Fig. 5*B*). LS174T colorectal cells were injected in mice, and once small tumors were established, animals were injected daily (2 $\times$ 5 days sequence) with meriolin 3 at a final concentration of 2 or 5 mg/kg. At the end of the experiment, meriolin 3 had induced 59% (5 mg/kg) or 40% (2 mg/kg) inhibition of tumor growth (Fig. 5*B*).

Discussion

Compared with terrestrial microorganisms and plants, marine organisms constitute a relatively untapped source of bioactive molecules. In recent years, however, an exponentially growing number of original structures derived from marine microorganisms, plants, and animals have been identified, some of which are reaching clinical stages and progressing to the pharmaceutical market (reviews in refs. 35–37).

We here report on meriolins, a family of kinase inhibitors designed from two different classes of marine natural products, the meridianins (Ascidian) and the variolins (Sponge). Meridianins had been reported as modest and rather unselective kinase inhibitors (11). Variolins have been extensively studied following the discovery of their potent antiproliferative and cell death–inducing properties. They are currently undergoing preclinical studies as potential antitumor agents (PharmaMar). As this work was in progress, variolin B and deoxyvariolin B were reported to inhibit

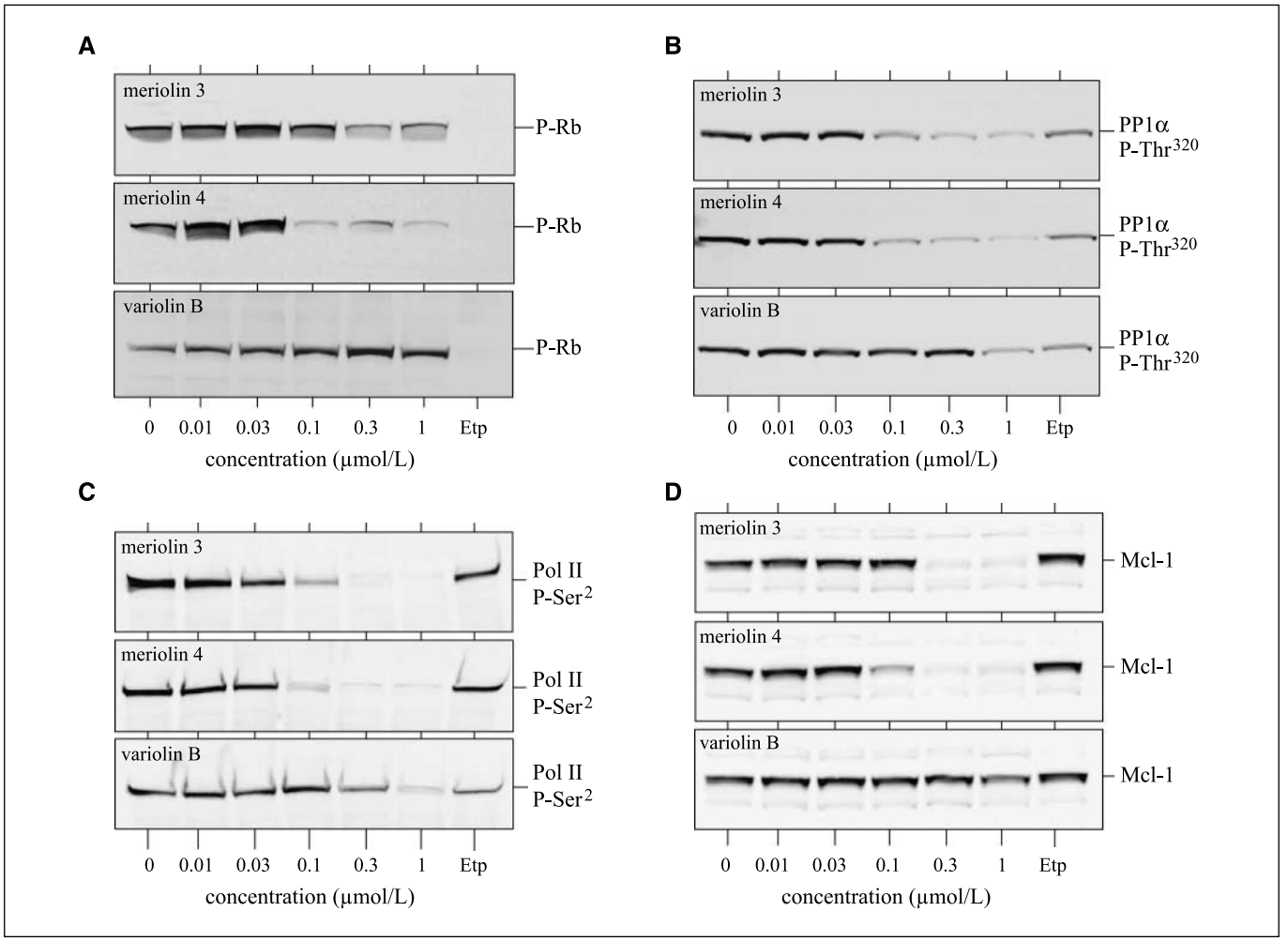

Figure 4. Inhibition of phosphorylation at CDK-specific sites and down-regulation of Mcl-1. SH-SY5Y cells were exposed to increasing concentrations of meriolin 3, meriolin 4, or variolin B for 24 h, and proteins were resolved by SDS-PAGE followed by Western blotting with antibodies phospho-Rb (*A*), phospho-Thr^{320} PP1α (*B*), phospho-Ser^2-RNA polymerase II (*C*), and Mcl-1 (*D*). Western blotting with anti-actin antibodies was used as a loading control (Supplementary Materials). *Etp,* etoposide, 12.5 μmol/L. Representative of two to three independent experiments.

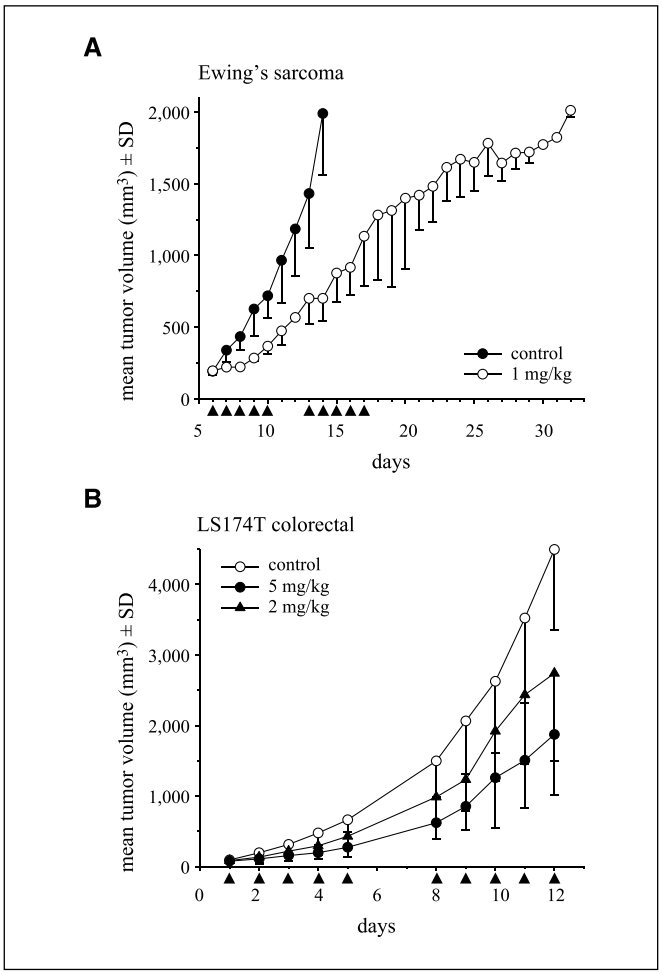

Figure 5. Antitumor activity of meriolin 3. *A,* meriolin 3 treatment of Ewing's sarcoma xenografts established in mice resulted in tumor growth delay. Xenografts established by s.c. inoculation of A4573 cells in nude mice were grown to a mean volume of about 195 mm^3. Animals carrying tumors were randomized into two groups. One group ($n = 6$) was treated with meriolin 3 in DMSO, given as single daily i.p. injections (*arrowheads*), at a dose of 1 mg/kg, for either 5 d or two 5-d series with a 2-d break in between. The control group ($n = 6$) received i.p. injections of DMSO following identical schedules. Results shown correspond to one of the experimental replicas using the two 5-d treatment schedule. *B,* Meriolin 3 treatment of LS174T colorectal carcinoma xenografts established in mice resulted in tumor growth delay. Xenografts established by s.c. inoculation of LS174T cells in nude mice were grown for 8 d. Animals carrying tumors were randomized into three groups. Two groups ($n = 5$) were treated with meriolin 3, given as single daily i.p. injections (*arrowheads*) at a dose of 2 or 5 mg/kg, for two 5-d series. The control group ($n = 5$) received i.p. injections of carrier following identical schedules.

CDK1, CDK2, and, to a lesser extent, CDK7 (23). We have confirmed these initial results and extended them to other CDKs and other kinases. Two other significant targets of variolin B are GSK-3 and CK1. In fact, variolin B is, to our knowledge, the most potent inhibitor of CK1 reported thus far. Variolin B analogues might thus be designed with high selectivity for CK1, a significant therapeutic target in both Alzheimer's disease (38) and cancer (39). When we analyzed its overall selectivity on a wider range of kinases (Fig. 1*C*), variolin seemed to act on many kinases, yet with preferred specificity toward CDK9 and FLT3 (Fig. 1). In contrast, meriolins seem to have clear target preference for CDKs, especially CDK2 and CDK9. To gain a more exhaustive view of the targets of meriolins, we are currently designing an affinity chromatography matrix bearing immobilized meriolin to purify its interacting proteins from cell and tissue extracts. This method has previously been employed to identify purvalanol- (40) and roscovitine-binding proteins (28) and should allow us to identify other potential kinase and nonkinase targets of meriolins.

The determination of structures for CDK2/cyclin A in complex with meriolin 3 and variolin B (Fig. 2) shed some light on the mechanisms of action of these molecules on their CDK target. Meriolins were initially designed by analogy to variolin B, and they do indeed make similar interactions with CDK2, notably making hydrogen bonds with Lys^{33}, Glu^{81}, and Leu^{83} within the ATP binding site. However, the crystal structures revealed that the two inhibitors adopt different orientations, resulting in the aza-indole ring and the 2-aminopyrimidine ring shared by both compounds occupying different binding sites (Fig. 2). A more detailed analysis of these co-crystal structures will be published elsewhere.[9]

Using various meriolins, and various cell models, we investigated the effects of meriolins on cell survival. Meriolins induced cell death at submicromolar concentrations in all cell lines tested, with the noticeable exception of normal fibroblasts, which were rather resistant (Table 1*B*). The most active meriolins were 3-fold more potent than variolin B (Table 1*A*). Extensive analysis of cell death mechanisms revealed that meriolins, like variolin B, induce classic apoptosis features, including the down-regulation of Mcl-1 (Fig. 4*D*), cytochrome *c* release from the mitochondria (Fig. 3*C*), activation of effector caspases (Fig. 3*D*), and ultimately cell death (LDH release, Fig. 3*B*).

The molecular mechanisms involved in meriolin-induced cell death remain to be characterized. Although meriolins inhibit CDK1 (Thr^{320} phosphorylation site on PP1α), CDK2 and CDK4 (Rb phosphorylation sites), we believe that CDK9 inhibition (monitored by Ser^2 phosphorylation on RNA polymerase II) constitutes the key event responsible for activation of the apoptotic pathway. There is indeed growing evidence supporting the role of CDK9 inhibition as an essential mechanism of action of CDK inhibitors in their antitumor-inducing activities (refs. 41, 42; reviewed in ref. 7). Inhibition of CDK9, a major regulator of RNA polymerase II, is expected to lead to the down-regulation of RNA polymerase II activity and, thus, to reduction in transcription. This is expected to preferentially affect short-lived proteins. Mcl-1, an antiapoptotic regulatory protein that couples cell survival to apoptosis (reviewed in refs. 43, 44), is such a high-turnover protein with an extremely short half-life (2–4 h). Through its ability to bind to Bim, Bak, Bax, and other Bcl-2 family members, it neutralizes these proapoptotic factors and thus acts as a key survival factor. Mcl-1 expression is highly regulated both at the transcriptional level (by transcription factors such as signal transducers and activators of transcription 3, cAMP-responsive element binding protein, PU.1) and at the translational level. Mcl-1 is also tightly regulated at the post-translational level both by proteosomal degradation following ubiquitinylation by MULE (45), an Mcl-1–specific E3 ligase, and by phosphorylation. Indeed, Mcl-1 is phosphorylated at various sites, leading either to stabilization (Thr^{163} phosphorylation by Erk; ref. 46), destabilization (Ser^{159} phosphorylation by GSK-3; ref. 47), or enhanced binding to proapoptotic factors Bim, Noxa, and Bak (Ser^{64} phosphorylation by CDK1, CDK2, c-jun-NH_2-kinase 1; ref. 48). Mcl-1 is highly expressed in tumor cells, but either at low concentrations or not at all in normal cells. Enhanced expression of Mcl-1 is observed in multiple cancers and is associated with poor prognostic and, thus, constitutes a significant anticancer drug target (reviewed in ref. 49).

We propose that meriolins act through at least three mechanisms: (*a*) by inhibiting CDK9, they transiently reduce both RNA polymerase II level (Supplementary Figure) and activity (Fig. 4*C*) and, consequently, down-regulate Mcl-1 expression levels (Fig. 4*D*); (*b*) by inhibiting CDK1, they reduce sequestering of proapoptotic factors by Mcl-1; and (*c*) by inhibiting CDK1 and CDK2, they block cell cycle progression both at the G_1-S and G_2-M transition, possibly leading to E2F-1–dependent apoptosis (41). As a consequence of Mcl-1 reduction and inhibition of its sink effects, proapoptotic regulators are liberated and trigger cell death. This CDK1/CDK2/CDK9 inhibition mechanism might be general for antitumor CDK inhibitors that are developed for clinical use against cancers (7, 41, 42).

Our results showed that meriolin 3 has potent antitumor activity. The A4573 Ewing's tumor xenograft model has been used previously to test the antitumor activity of roscovitine, another CDK inhibitor (31). In this regard, it seems that, in this xenograft model system with the same type of treatment schedule, meriolin 3 is a more potent inhibitor of tumor growth than roscovitine. At the time control animals had to be sacrificed to follow institutional tumor burden guidelines, roscovitine had caused an ~85% inhibition of tumor growth (39), whereas meriolin 3 had an ~65% inhibition. However, it is important to point out that roscovitine was used at a concentration 50-fold higher than that of meriolin 3 (50 mg/kg versus 1 mg/kg, respectively), indicating that meriolin 3 is still ~40-fold more efficient at inhibiting the growth of Ewing's sarcoma xenografts and strongly suggesting that meriolin 3 may be an effective cancer therapeutic agent. Similar promising *in vivo* antitumor effects were observed with low concentrations of meriolin 3 using LS174T colorectal carcinoma in nude mice. These experiments are only exploratory; meriolins need to be optimized, and their administration needs to be explored further with respect to dosing, timing, and combination with other drugs. Nevertheless, this family of small-molecular-weight compounds, derived from marine natural products, as pharmacologic inhibitors of CDKs, display promising antitumor activity that requires further studies.

Acknowledgments

Received 5/17/2007; revised 7/3/2007; accepted 7/11/2007.

Grant support: EEC (FP6-2002-Life Sciences & Health, PRO-KINASE Research Project; L. Meijer, M. Kubbutat, and J. Endicott), "Cancéropole Grand-Ouest" grant (L. Meijer and S. Marionneau-Lambot), the Australian Research Council (J.C. Morris), and US NIH grant PO1-CA74175 (O.M. Tirado and V. Notario). K. Bettayeb was supported by a fellowship from the Ministère de la Recherche.

The costs of publication of this article were defrayed in part by the payment of page charges. This article must therefore be hereby marked *advertisement* in accordance with 18 U.S.C. Section 1734 solely to indicate this fact.

This article is dedicated to Dr. George R. Pettit, a pioneer in anticancer marine natural products, with friendship and respect. We are grateful to Dr. M. Clement for providing the cell survival data for GBM cells and KMS-11 cells, to Dr. G. Ponzio for the human foreskin primary fibroblasts, to C. Guillouzo and J. Boix for cell lines, and to the beamline scientists at the ESRF (ID14-2) for providing excellent facilities for crystal data collection.

References

1. Noble ME, Endicott JA, Johnson LN. Protein kinase inhibitors: insights into drug design from structure. Science 2004;303:1800–5.
2. Weinmann H, Metternich R. Drug discovery process for kinase inhibitors. Chembiochem 2005;6:455–9.
3. Malumbres M, Barbacid M. Mammalian cyclin-dependent kinases. Trends Biochem Sci 2005;30:630–41.
4. Knockaert M, Greengard P, Meijer L. Pharmacological inhibitors of cyclin-dependent kinases. Trends Pharmacol Sci 2002;23:417–25.
5. Fischer PM, Gianella-Borradori A. Recent progress in the discovery and development of cyclin-dependent kinase inhibitors. Exp Opin Investig Drugs 2005;14:457–77.
6. Misra RN. Clinical progress of selective cyclin-dependent kinase (CDK) inhibitors. Drugs Future 2006;31:43–52.
7. Shapiro GI. Cyclin-dependent kinase pathways as targets for cancer treatment. J Clin Oncol 2006;24:1770–83.
8. Smith PJ, Yue E, editors. CDK inhibitors of cyclin-dependent kinases as anti-tumor agents. Monographs on enzyme inhibitors, vol. 2. Boca Raton, Taylor & Francis, 2006; 448 pp.
9. Bach S, Blondel M, Meijer L. Evaluation of CDK inhibitors' selectivity: from affinity chromatography to yeast genetics. In E. Yue and P.J. Smith, editors. Monographs on enzyme inhibitors, vol. 2. CDK inhibitors and their potential as anti-tumor agents. CRC Press, Taylor & Francis, chapter 5, 2006, p. 103–19.
10. Leclerc S, Garnier M, Hoessel R, et al. Indirubins inhibit glycogen synthase kinase-3β and CDK5/p25, two kinases involved in abnormal tau phosphorylation in Alzheimer's disease—a property common to most CDK inhibitors? J Biol Chem 2001;276:251–60.
11. Gompel M, Leost M, Bal de Kier Joffe E, et al. Meridianins, a new family of protein kinase inhibitors isolated from the Ascidian *Aplidium meridianum*. Bioorg Med Chem Lett 2004;14:1703–7.
12. Franco LH, Bal de Kier Joffe E, Puricelli L, Tatian M, Seldes AM, Palermo JA. Indole alkaloids from the tunicate *Aplidium meridianum*. J Nat Prod 1998;61:1130–2.
13. Fresneda PM, Molina P, Delgado S, Bleda JA. Synthetic studies towards the 2-aminopyrimidine alkaloids variolins and meridianins from marine origin. Tetrahedron Lett 2000;41:4777–80.
14. Jiang B, Yang CG. Synthesis of indolylpyrimidines via cross-coupling of indolylboronic acid with chloropyrimidines: facile synthesis of meridianin D. Heterocycles 2000;53:1489–98.
15. Franco LH, Palermo JA. Synthesis of 2-(pyrimidin-4-yl)indoles. Chem Pharm Bull 2003;51:975–7.
16. Perry NB, Ettouati L, Litaudon M, et al. Alkaloids from the Antarctic sponge *Kirkpatrickia varialosa*. Part 1: variolin B, a new antitumour and antiviral compound. Tetrahedron 1994;50:3987–92.
17. Trimurtulu G, Faulkner DJ, Perry NB, et al. Alkaloids from the Antarctic sponge *Kirkpatrickia varialosa*. Part 2: variolin A and *N*(3′)-methyl tetrahydrovariolin B. Tetrahedron 1994;50:3993–4000.
18. Anderson RJ, Morris JC. Total synthesis of variolin B. Tetrahedron Lett 2001;42:8697–9.
19. Anderson RJ, Hill JB, Morris JC. Concise total syntheses of variolin B and deoxyvariolin B. J Org Chem 2005;70:6204–12.
20. Molina P, Fresneda PM, Delgado S. Carbodiimide-mediated preparation of the tricyclic pyrido[3′,2′:4,5]-pyrrolo[1,2-*c*]pyrimidine ring system and its application to the synthesis of the potent antitumoral marine alkaloid variolin B and analog. J Org Chem 2003;68:489–99.
21. Ahaidar A, Fernandez D, Danelon G, et al. Total syntheses of variolin B and deoxyvariolin B. J Org Chem 2003;68:10020–9.
22. Erba E, Balconi G, Faretta M. et al. 1996. Cell cycle phase perturbation and apoptosis induced by variolin B, a novel antitumor agent of marine origin. Proc Am Ass Cancer Res 1996;37:28.
23. Simone M, Erba E, Damia G, et al. Variolin B and its derivate deoxy-variolin B: new marine natural compounds with cyclin-dependent kinase inhibitor activity. Eur J Cancer 2005;41:2366–77.
24. Brown NR, Noble ME, Endicott JA, Johnson LN. The structural basis for specificity of substrate and recruitment peptides for cyclin-dependent kinases. Nat Cell Biol 1999;1:438–43.
25. Collaborative Computational Project, Number 4. The CCP4 suite: programs for protein crystallography. Acta Cryst 1994;D50:760–3.
26. Emsley P, Cowtan K. Coot: model-building tools for molecular graphics. Acta Cryst 2004;D60:2126–32.
27. Murshudov GN, Vagin AA, Dodson EJ. Refinement of macromolecular structures by the maximum-likelihood method. Acta Cryst 1997;D53:240–55.
28. Bach S, Knockaert M, Lozach O, et al. Roscovitine targets: protein kinases and pyridoxal kinase. J Biol Chem 2005;280:31208–19.
29. Reinhardt J, Ferandin Y, Meijer L. Purification of native, active casein kinase 1 (CK1) by affinity chromatography on immobilised axin fragment. Protein Expr Purif 2007;54:101–9.
30. Ribas J, Bettayeb K, Ferandin Y, et al. 7-bromoindirubin-3′-oxime induces caspase-independent cell death. Oncogene 2006;25:6304–18.
31. Tirado OM, Mateo-Lozano S, Notario V. Roscovitine is an effective inducer of apoptosis of Ewing's sarcoma family tumor cells *in vitro* and *in vivo*. Cancer Res 2005;65:9320–7.
32. Zarkowska T, Mittnacht S. Differential phosphorylation of the retinoblastoma protein by G_1-S cyclin-dependent kinases. J Biol Chem 1997;272:12738–46.
33. Kwon YG, Lee SY, Choi Y, Greengard P, Nairn AC. Cell cycle-dependent phosphorylation of mammalian protein phosphatase 1 by cdc2 kinase. Proc Natl Acad Sci U S A 1997;94:2168–73.
34. Payton M, Chung G, Yakowec P, et al. Discovery and evaluation of dual CDK1 and CDK2 inhibitors. Cancer Res 2006;66:4299–308.
35. Nakao Y, Fusetani N. Enzyme inhibitors from marine invertebrates. J Nat Prod 2007;70:689–710.
36. Newman DJ, Cragg GM. Marine natural products and related compounds in clinical and advanced preclinical trials. J Nat Prod 2004;67:1216–38.
37. Blunt JW, Copp BR, Hu WP, Munro MHG, Northcote PT, Prinsep MR. Marine natural products. Nat Prod Rep 2007;24:31–86.
38. Flajolet M, He G, Heiman M, Lin A, Nairn AC, Greengard P. Regulation of Alzheimer's disease amyloid-β formation by casein kinase I. Proc Natl Acad Sci U S A 2007;104:4159–64.

39. Knippschild U, Wolff S, Giamas G, et al. The role of the casein kinase 1 (CK1) family in different signaling pathways linked to cancer development. Onkologie 2005;28:508–14.
40. Knockaert M, Gray N, Damiens E, et al. Intracellular targets of cyclin-dependent kinase inhibitors: identification by affinity chromatography using immobilised inhibitors. Chem Biol 2000;7:411–22.
41. Cai D, Byth KF, Shapiro GI. AZ703, an imidazo[1,2-*a*]pyridine inhibitor of cyclin-dependent kinases 1 and 2, induces E2F-1–dependent apoptosis enhanced by depletion of cyclin-dependent kinase 9. Cancer Res 2006; 66:435–44.
42. Cai D, Latham VM, Jr., Zhang X, Shapiro GI. Combined depletion of cell cycle and transcriptional cyclin-dependent kinase activities induces apoptosis in cancer cells. Cancer Res 2006;66:9270–80.
43. Yang-Yen HF. Mcl-1: a highly regulated cell death and survival controller. J Biomed Sci 2006;13:201–4.
44. Adams JM, Cory S. The Bcl-2 apoptotic switch in cancer development and therapy. Oncogene 2007;26:1324–37.
45. Zhong Q, Gao W, Du F, Wang X. Mule/ARF-BP1, a BH3-only E3 ubiquitin ligase, catalyzes the polyubiquitination of Mcl-1 and regulates apoptosis. Cell 2005;121:1085–95.
46. Domina AM, Vrana JA, Gregory MA, Hann SR, Craig RW. MCL1 is phosphorylated in the PEST region and stabilized upon ERK activation in viable cells, and at additional sites with cytotoxic okadaic acid or taxol. Oncogene 2004;23:5301–15.
47. Maurer U, Charvet C, Wagman AS, Dejardin E, Green DR. Glycogen synthase kinase-3 regulates mitochondrial outer membrane permeabilization and apoptosis by destabilization of MCL-1. Mol Cell 2006;21:749–60.
48. Kobayashi S, Lee SH, Meng XW, et al. Serine 64 phosphorylation enhances the antiapoptotic function of Mcl-1. J Biol Chem 2007;282:18407–17.
49. Mandelin AM II, Pope RM. Myeloid cell leukemia-1 as a therapeutic target. Expert Opin Ther Targets 2007;11: 363–73.